



# Beryllium abundances and the early Galactic chemical enrichment

Rodolfo Smiljanic<sup>1</sup>

1) Nicolaus Copernicus Astronomical Center, Polish Academy of Sciences, Warsaw, Poland  
(rsmiljanic@camk.edu.pl)



## INTRODUCTION

Beryllium is a light element with a single stable isotope, <sup>9</sup>Be, which can only be produced by cosmic-ray spallation. In old, metal-poor stars there is a linear relation between the abundance of Be and metallicity (see Fig. 1 and, e.g., Boesgaard et al. 2009; Smiljanic et al. 2009).

However, the continuity of the linear relation down to the extremely metal-poor regime (around and below  $[Fe/H] \sim -3.0$ ) has been subject to some discussion. Primas et al. (2000a,b) were the first to explore this metallicity regime and found a possible deviation from the linear relation (i.e., a flattening) below  $[Fe/H] \sim -3.0$ .

The evidence supporting the flattening of the relation was made weaker by a few upper limits at very low metallicities ( $[Fe/H] \sim -3.7$ ) determined by Ito et al. (2009) and Spite et al. (2019). Nevertheless, we showed in Smiljanic et al. (2021) that indeed there is an increase in the scatter at this metallicity regime.

In this work, we are extending the Smiljanic et al. (2021) results with stars up to  $[Fe/H] \sim -2.0$ . We are trying to investigate at which metallicity the scatter disappears and the linear relation between Be and Fe becomes well behaved.

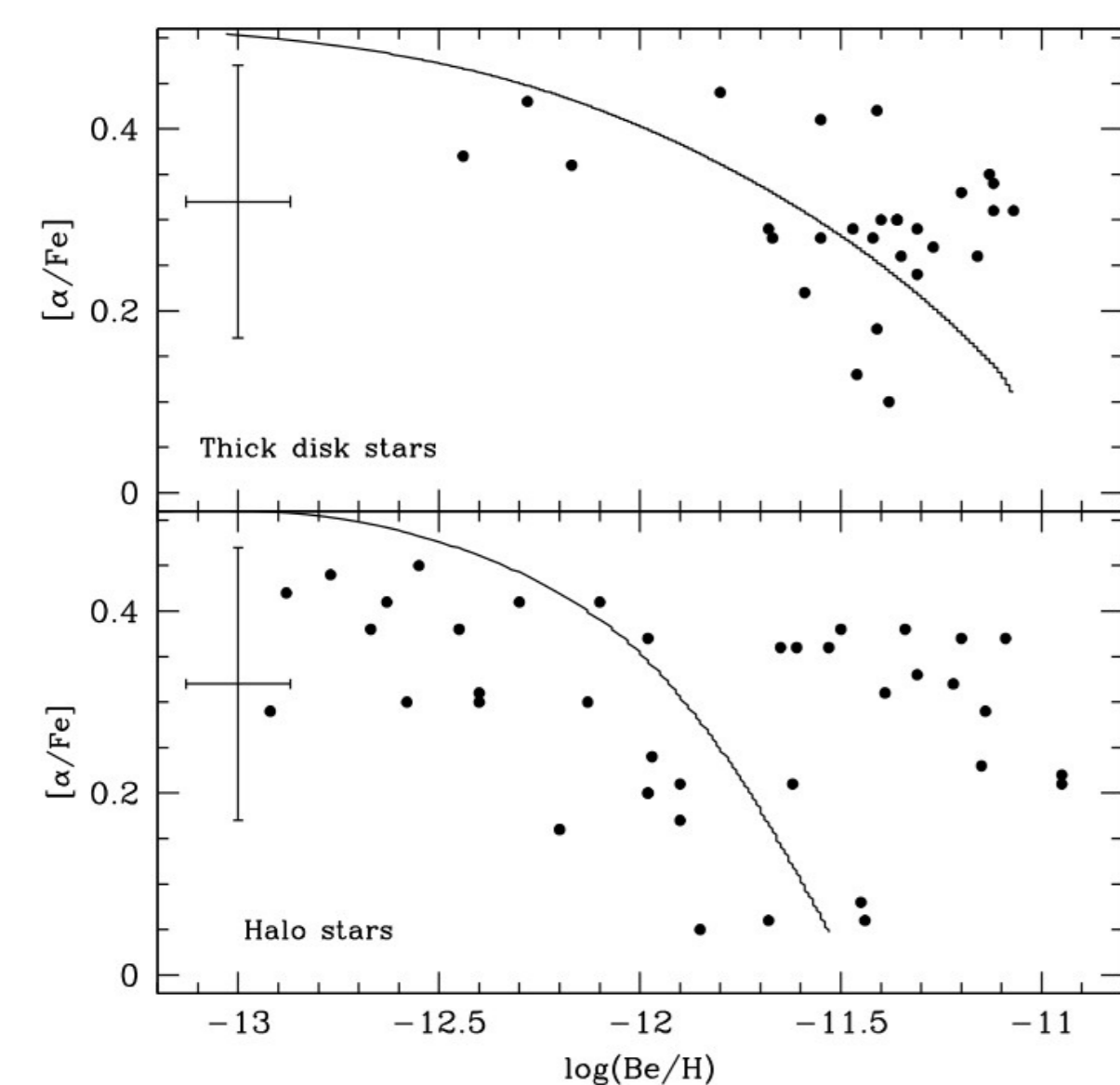


Fig. 1 -  $[\alpha/Fe]$  as a function of  $\log(Be/H)$  from the work of Smiljanic et al. (2009). The halo stars clearly divide into two sequences, where the one of low  $[\alpha/Fe]$  is likely an accreted stellar population.

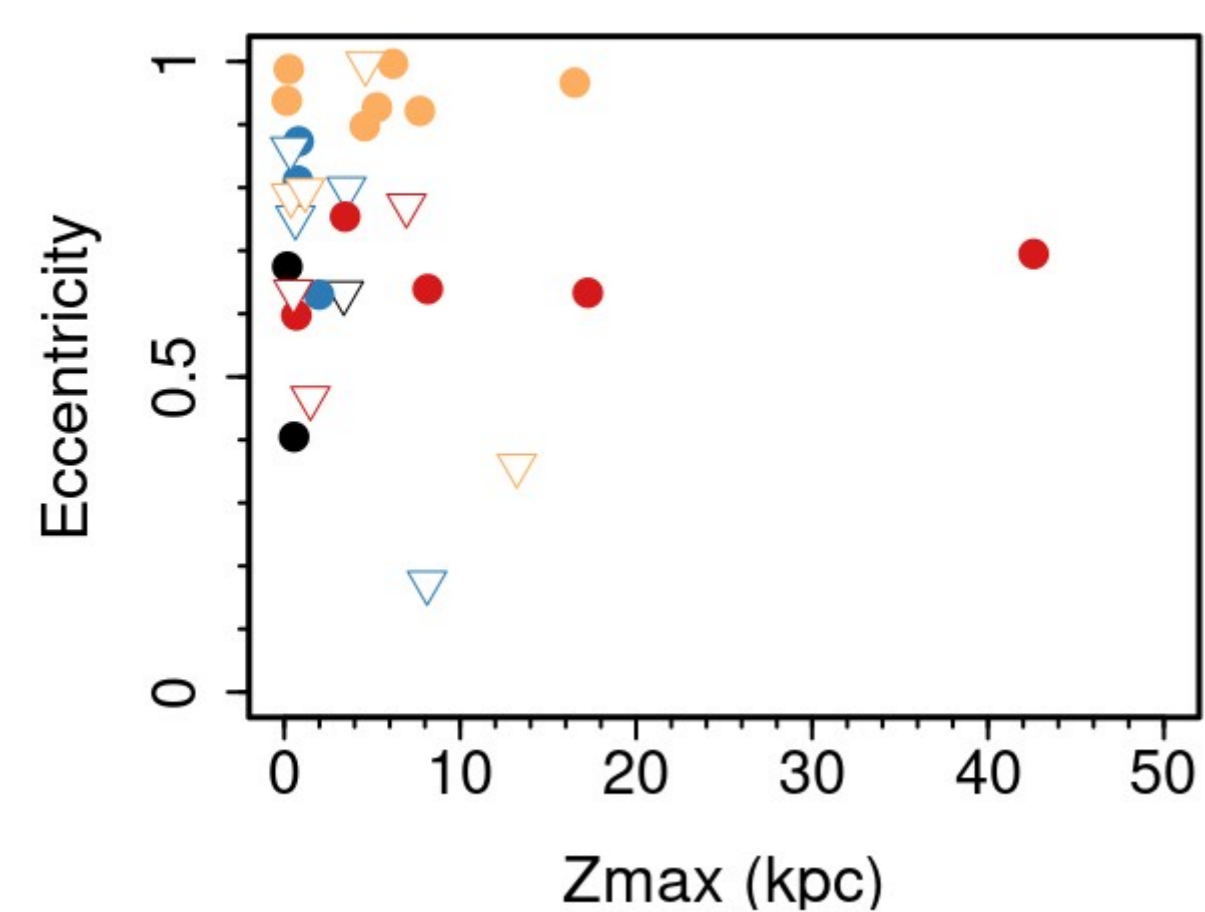


Fig. 4 - Orbital eccentricity as a function of  $Z_{max}$  (maximum distance the star reaches from the Galactic plane in its orbit). Symbols are as discussed before. At least 1 star with  $Z_{max} > 40$  kpc is likely part of the outer halo population.

## STELLAR POPULATIONS

We classify the stars to Galactic stellar populations using their velocities and orbital parameters.

Three stars with total velocity below 200 km/s are considered to be likely disc stars (shown in black in the plots of this and following panels). Stars with total velocity between 200-230 km/s are considered to be part of the heated disc (or inner halo); these stars are shown in blue in the plots of this and following panels. To classify stars as part of Gaia-Enceladus (Helmi et al. 2018), we use the criteria based on energy and angular momentum from Massari et al. (2019); see Lindblad diagram in the following panel. Stars that likely belong to Gaia-Enceladus are shown as orange symbols. Finally, other retrograde stars that do not belong to Gaia-Enceladus are shown as red symbols.

## Be IN THE EARLY GALAXY

Pasquini et al. (2005) showed that different Galactic kinematic stellar populations (the accretion and dissipative components, see Gratton et al. 2003) could be separated in a diagram of  $[O/Fe]$  as a function of  $\log(Be/H)$ .

Afterwards, Smiljanic et al. (2009) found that the halo stars are the ones to divide into two different sequences in a plot of  $[\alpha/Fe]$  as a function of  $\log(Be/H)$ . They suggested the division was a sign of either an accreted stellar component or of variations in the star formation history in initially independent regions of the early halo.

Molaro et al. (2020) showed that the mixture of stars from Gaia-Enceladus with those formed in-situ could be the reason for the observed scatter in a diagram of  $\log(Be/H)$  versus  $[Fe/H]$ . This was expanded to the extremely metal-poor regime by Smiljanic et al. (2021).

Our interpretation however is abundances of Fe, and not those of Be, drive the scatter. In other words, that at the time of the formation of the early halo, Fe abundances (in a Galactic context) were more inhomogeneous than the Be abundances. The co-existence of in-situ and accreted stars at this regime, clearly shows that this mix of stellar populations plays a role in the observed scatter.

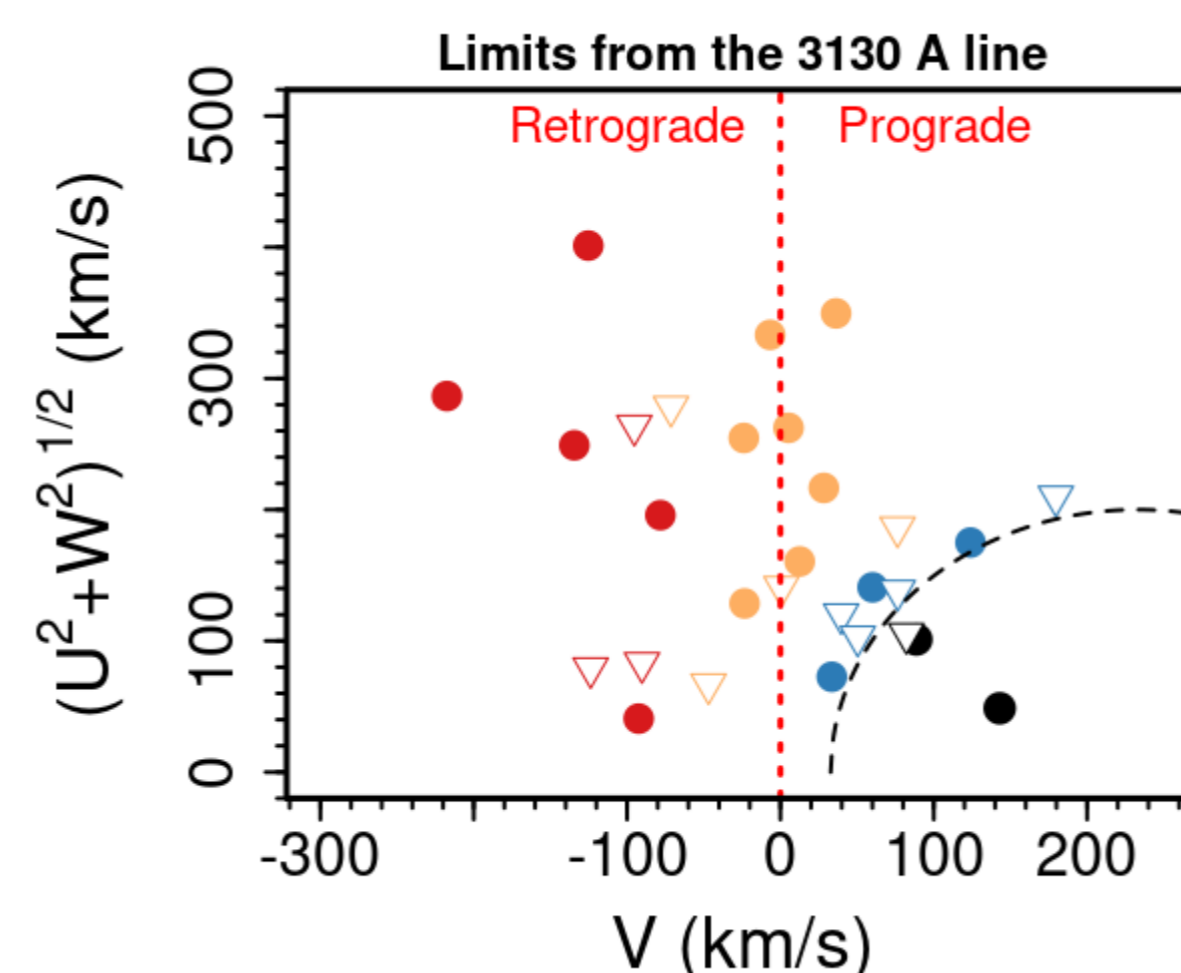


Fig. 2 - Toomre diagram for the sample from Smiljanic et al. (2021) complemented with the 12 new stars analysed here. Symbols are related to the Be abundance derived from the line at 3130 Å (solid circle for detection, open triangle for upper limit). Colors are related to stellar population (black likely disc, blue likely heated disc, orange likely Gaia-Enceladus, and red likely other accreted stars - see explanation below).

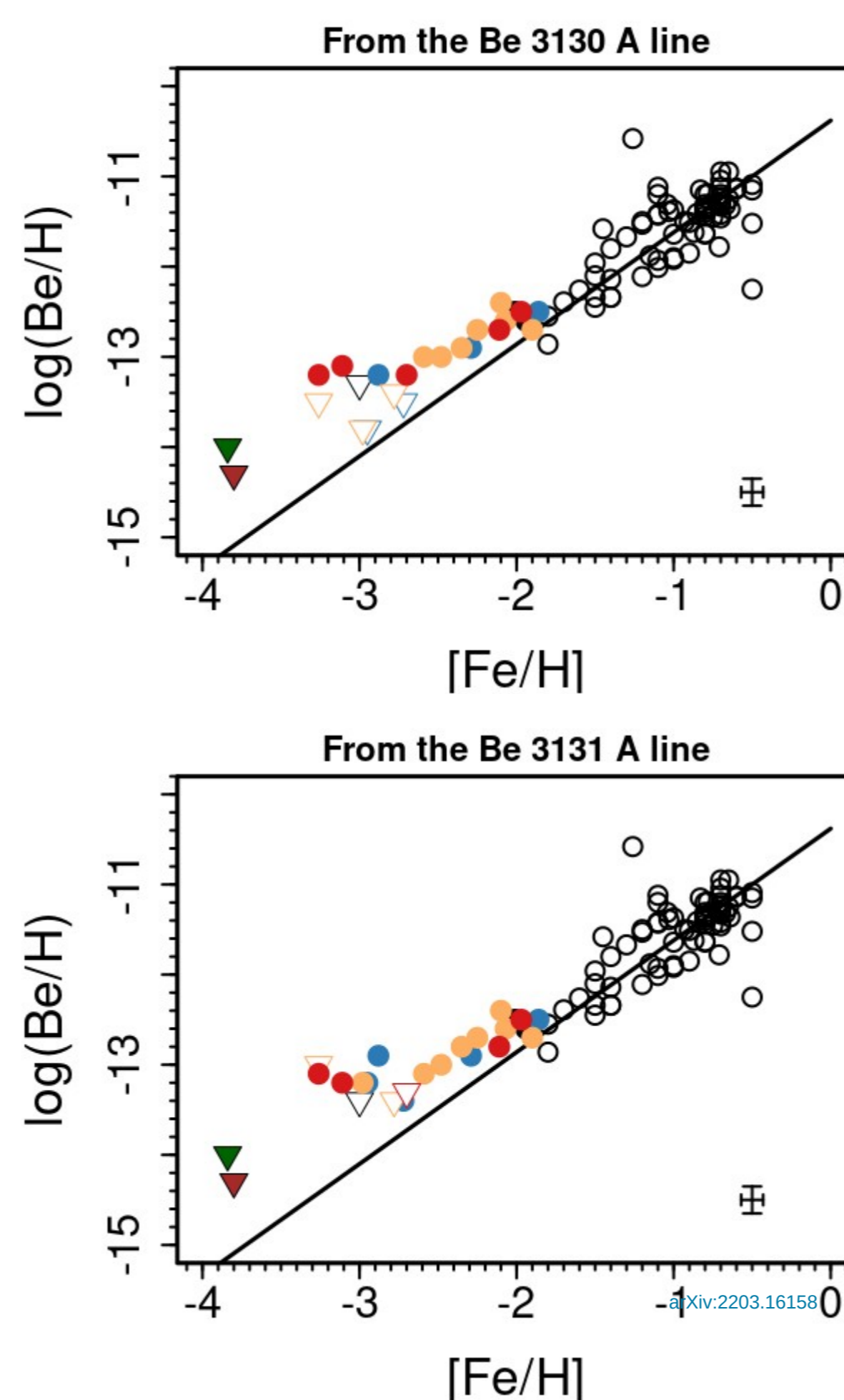


Fig. 5 - Be abundances as a function of metallicity. Open circles are stars from Smiljanic et al. (2009). The upper limits for stars 2MASS J18082002-5104378 (Spite et al. 2019) and BD+44 493 (Placco et al. 2014) are shown as upside-down dark green and brown triangles. The stars from Smiljanic et al. (2021) and from this work are shown in black (disc), blue (heated disc), orange (Gaia-Enceladus), and red (other accreted populations). Abundances from each Be line, at 3130 and 3131 Å, are shown separately (see why in Smiljanic et al. 2021).

## DATA AND ANALYSIS

In this work, we present preliminary results of an extension of the Smiljanic et al. (2021) results. We increase the sample to include 12 stars with up to  $[Fe/H] \sim -2.0$  and try to classify them according to membership in the different populations at this metallicity (i.e., accreted populations, heated disc, metal-weak thick disc, etc).

All spectra used in this analysis were obtained using the Ultraviolet and Visual Echelle Spectrograph (UVES, Dekker et al. 2000), fed by the Unit Telescope 2 of the Very Large Telescope (VLT) of the European Southern Observatory (ESO) at Cerro Paranal, Chile.

Beryllium abundances were determined with spectrum synthesis using Turbospectrum (Plez 2012) and MARCS model atmospheres (Gustafsson et al. 2008). The line list is that assembled in Smiljanic et al. (2022) and Giribaldi & Smiljanic (2022) for tests during the Phase A study of the CUBES spectrograph (Zanutta et al. 2022).

We made use of Gaia DR3 (Vallenari et al. 2022) parallaxes and proper motions to compute stellar velocities and orbits. We integrated the orbits of the stars in the Galaxy using code GalPot of McMillan (2017).

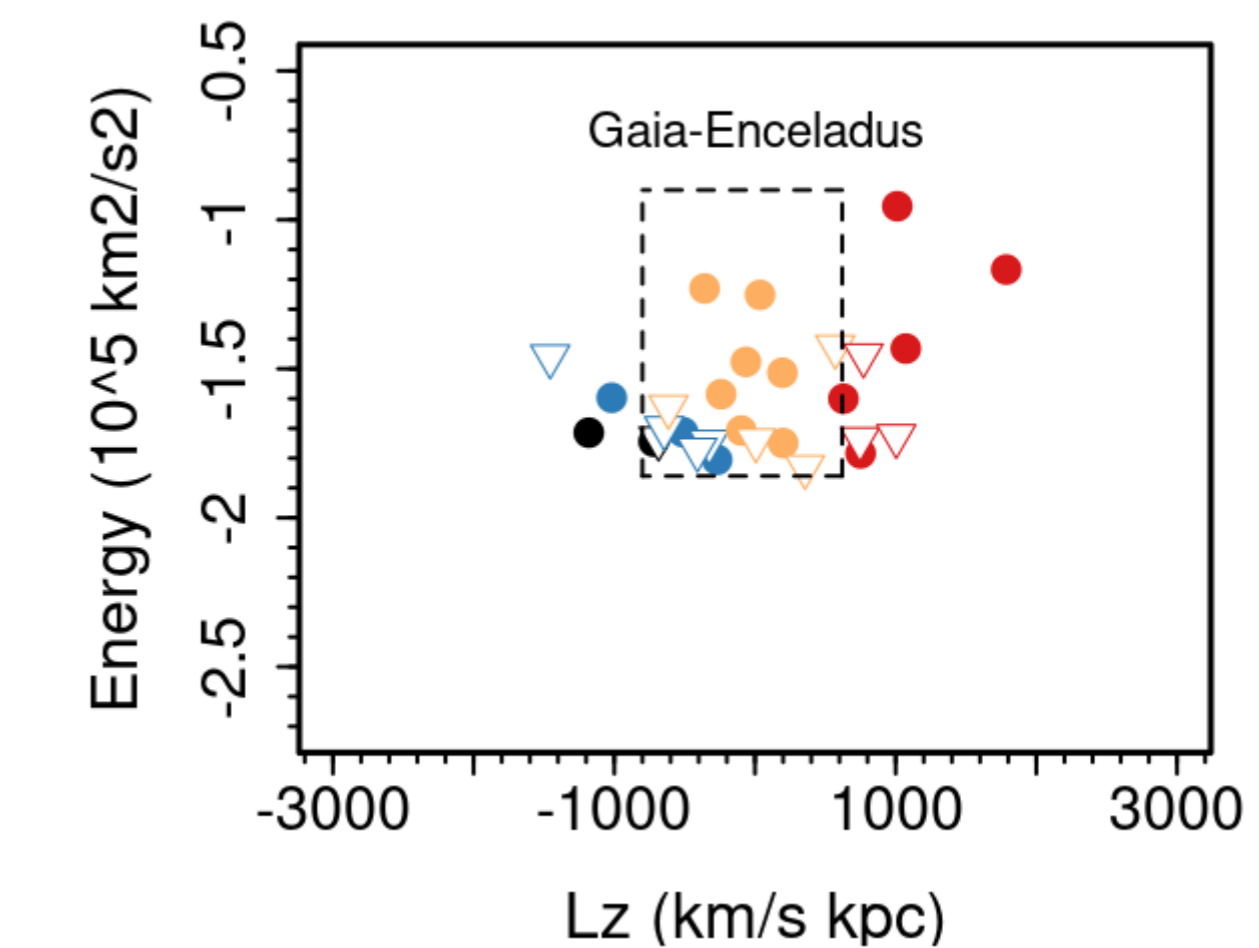


Fig. 3 - Linblad diagram (orbital energy as a function of the angular momentum in the Z direction). Stars inside the box, that were not classified as likely disc or heated disc stars using the Toomre diagram, are considered to be likely members of Gaia-Enceladus.

## DISCUSSION

The idea that abundances of Be (and of other cosmic-ray spallation products) can have smaller scatter when compared to abundances of elements produced by stellar nucleosynthesis was first suggested by the results of Suzuki et al. (1999) and Suzuki & Yoshii (2001). These authors computed chemical evolution models of an inhomogeneous early Galactic halo. Based on these models, Be abundances were suggested to be a good cosmochronometer for the early stages of the Galaxy (Beers et al. 2000; Suzuki & Yoshii 2001).

If that interpretation is correct, investigating the scatter in the relation between Be and Fe to higher metallicities, could reveal at which point the ISM becomes more homogeneous. The new stars added to our sample, all with  $[Fe/H] > -3$  and  $< -1.9$ , show much less scatter than what was observed in the extremely metal-poor regime. It seems that the ISM changes from inhomogeneous to homogeneously mixed somewhere around  $[Fe/H] \sim -2.6$  or  $\log(Be/H) > -13.0$ .

## REFERENCES

- Beers et al. 2000, IAU Symp., 198, 425
- Boesgaard et al. 2011, ApJ, 743, 140
- Dekker et al. 2002, SPIE Conf. Ser., 4008, 534
- Giribaldi & Smiljanic 2022, ExA accepted, arXiv:2203.15604
- Gratton et al. 2003, A&A, 406, 131
- Gustafsson et al. 2008, A&A, 486, 951
- Helmi et al. 2018, Nature, 563, 85
- Ito et al. 2009, ApJ, 698, L37
- Massari et al. 2019, A&A, 630, L4
- McMillan et al. 2017, MNRAS, 465, 76
- Molaro et al. 2020, MNRAS, 496, 2902
- Pasquini et al. 2005, A&A, 436, L57
- Placco et al. 2014, ApJ, 790, 34
- Plez 2012, Turbospectrum: Code for Spectral Synthesis
- Primas et al. 2000a, A&A, 364, L42
- Primas et al. 2000b, A&A, 362, 666
- Smiljanic et al. 2009, A&A, 499, 103
- Smiljanic et al. 2021, A&A, 646, A70
- Smiljanic et al. 2022, ExA accepted, arXiv:2203.16158
- Spite et al. 2019, A&A, 624, A44
- Suzuki et al. 1999, ApJ, 522, L125
- Suzuki & Yoshii 2001, ApJ, 549, 303
- Vallenari et al. 2022, A&A accepted
- Zanutta et al. 2022, ExA accepted, arXiv:2203.15352